Journal of Petroleum Research and Studies

journal homepage: https://jprs.gov.iq/index.php/jprs/

Print ISSN 2220-5381, Online ISSN 2710-1096

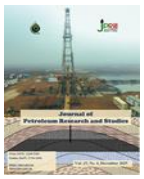

Carbon Dioxide Sequestration in Subsurface Formations to Enhance Hydrocarbon Recovery: Field Case Study from Southern Iraq

Mahdi M. Kadhim[1,2*], Hassan A. Abdul Hussein[1], Hayder L. Abdulridha[2]

[1]Petroleum Department, College of Engineering, University of Baghdad, Baghdad, Iraq.

[2]Thi Qar Oil Company, Ministry of Oil, Thi Qar, Iraq.

[*]Corresponding Author E-mail: mahdi.jawad2208m@coeng.uobaghdad.edu.iq

Article Info

Received 05/06/2024
Revised 26/06/2024
Accepted 01/12/2024
Published 21/12/2025

DOI:
http://doi.org/10.52716/jprs.v15i4.975

Abstract

Concern about reducing greenhouse gas emissions particularly those of carbon dioxide has developed along with an understanding of global warming and climate change and joined with enhanced oil recovery. Thus, research on improved oil recovery and supporting reservoir pressure utilizing greenhouse gases has been conducted throughout the last few decades.

The current study focuses on achieving the oil production target from the X oil field. It is located in southern Iraq; this field is thought to be the Y formation; planned by National Oil Company with CO_2 miscible gas injection and test the possibility of applied sequestration of CO_2 in the aquifer as reduced emission project. Building a 3D dynamic model with CMG-2018 based on a geological model exported from Petrel employed to investigate distinct developing plans with varying operational constraints. The compositional simulator (GEM-2018) is used to model Y formation. The model was calibrated with W-4 well testing because of a lack of production data.

The production case scenario has been suggested to develop Y formation as the preferred case based on the height recovery factor. The best case is the five-spot CO_2 injection with a plateau of 30 Kbbl/d for twenty years with production above the bubble point and with stored CO_2 of 5.75 MMTon in the S21 and exploiting the three abandoned to stored CO_2 of 3.265 MMTon in the aquifer as soluble emission gas.

Keywords: CCUS, CO2 Injection, CO2-EOR, CCS-EOR.

حقن ثنائي أوكسيد الكاربون في التكوينات التحت سطحية لتحسين استخلاص الهيدروكربون: دراسة حقلية في جنوب العراق

الخلاصة:

تطور الاهتمام بشأن الحد من انبعاثات الغازات الدفيئة وخاصة غاز ثاني أكسيد الكربون جنبًا إلى جنب مع فهم ظاهرة الاحتباس الحراري وتغير المناخ وتم ربط هذا الاهتمام إلى تعزيز استخراج النفط وهكذا، فقد تم إجراء أبحاث حول تحسين استخلاص النفط ودعم الضغط المكمني باستخدام الغازات الدفيئة طوال العقود القليلة الماضية.

تم في الدراسة الحالية التركيز على تحقيق هدف إنتاج النفط المخطط تحقيقه من قبل شركة نفط الوطنية من حقل X النفطي الذي يقع في جنوب العراق؛ من خلال تكوين نهر عمر (Y)، وذلك بحقن غاز ثاني أكسيد الكربون القابل للامتزاج وكذلك اختبار إمكانية استخدام المستودع المائي لمكمن Y كمستودع لتخزين غاز ثنائي أوكسيد الكاربون الذائب كمشروع لتقليل الانبعاثات.

تم بناء نموذج مكمني ثلاثي الأبعاد باستخدام CMG-2018 بناءً على الموديل جيولوجي الذي تم تصديره في المرحلة الاولى يُستخدم لدراسة خطط تطوير وادائية المكمن خلال قيود تشغيلية مختلفة. تم استخدام جهاز المحاكاة التركيبي (GEM-2018) لنمذجة تشكيلY . تمت معايرة النموذج بنتائج فحص البئر W-4 والإنتاج التراكمي.

أخيرًا، تم اقتراح سيناريو مكون من ست حالات لتطوير مكمن Y وتكون الحالة المفضلة بناءً على انتاج اعلى كمية من النفط. أفضل حالة هي حقن ثاني أكسيد الكربون من خلال طريقة الحقن الخماسية مع ثبات الانتاج بمعدل 30 ألف برميل في اليوم لمدة عشرين عامًا بضغط أعلى من ضغط نقطة الفقاعة بالإضافة الى تخزين غاز ثاني أكسيد الكربون بمقدار 5.75 مليون طن في طبقة S21 وكذلك استخدام الابار المهجورة الثلاثة لغرض حقن غاز ثاني أكسيد الكربون المذاب في الماء بمقدار 3.265 مليون طن.

1. Introduction

The most popular technique for better oil recovery is CO_2 injection. To reduce CO_2 emissions, CO_2 storage and enhanced oil production can be employed together [1,2]. In most cases, the reservoir oil is produced during the tertiary recovery process using compositions of hydrocarbon gases or pure CO_2 [3]. Since oil reservoirs are known to have a geologic seal that has allowed them to hold onto liquid and gas hydrocarbon for millions of years, it is attractive as a potential storage location [4]. One viable option for immediate action has been to inject CO_2 into oil reservoirs to achieve improved oil recovery (CO_2 EOR). This will generate a profit to offset the cost of CO_2 capture and storage [5].

The computations of the fluid flow among the grid blocks, fluid saturations, and pressures of each grid block are among the equations needed to create a model [6]; however, a compositional model more accurately captures the impact of phase behavior on the fluid displacement characteristics than a black oil model. The properties of the oil alter and it becomes more mobile when CO_2 comes into touch with the oil in the reservoir [7]. The oil is also forced to migrate in the direction of the producing well by the CO_2 that is injected. Most of the CO_2 that is injected is held inside the reservoir pores, but some of it is also created when the oil rises to the surface [8]. A closed-loop system is created when CO_2 is extracted from the oil and reinjected into the reservoir from the surface [9]. One alternative for storing the CO_2 that is extracted from the oil is to inject it into the underlying aquifer [10,11].

A screening process must be carried out before beginning any EOR project on an oil reservoir. Each screening criterion is composed of two parts: the technical and the economical. For an EOR project to be evaluated, both of these elements are essential. The miscible gas injection screening criteria are displayed in Table (1) Screening criteria for application of CO_2 miscible flood suggested by [12,13].

Table (1): Screening Criteria for the Application of CO_2 Miscible Flood [12,13]

Characteristics	**Kang, 2016**	**Green and Willhite ,1998**	Y reservoir **Properties**
API	> 22	> 22	28.8
Viscosity (cp)	<= 6	< 10	1.635
Formation type	-	Sandstone/carbonate	Sandstone
Depth (ft)	-	>2500	8200
Temperature (F)	-	Not critical	181.04
Permeability (md)	Homogeneous	Not critical	1740

The screening criteria previously described were the basis for this investigation, and the Y reservoir in the X field was selected to use the miscible injection of the gas method with CO_2. This work's primary objective was to offer the most effective way for raising layer S21 conformance control in the Y Formation, X Field, and improving the sweeps of miscible CO_2 floods and sequestration of CO_2 in the water.

1.1. Area of Study

X field situated in southern Iraq, as shown in Figure (1). The oil field is 30 km long and about 7 km wide. The Y sandstone formation is considered to be one of the most prolific reservoirs in southern Iraqi fields; the oil produced there has an API of 28.8.

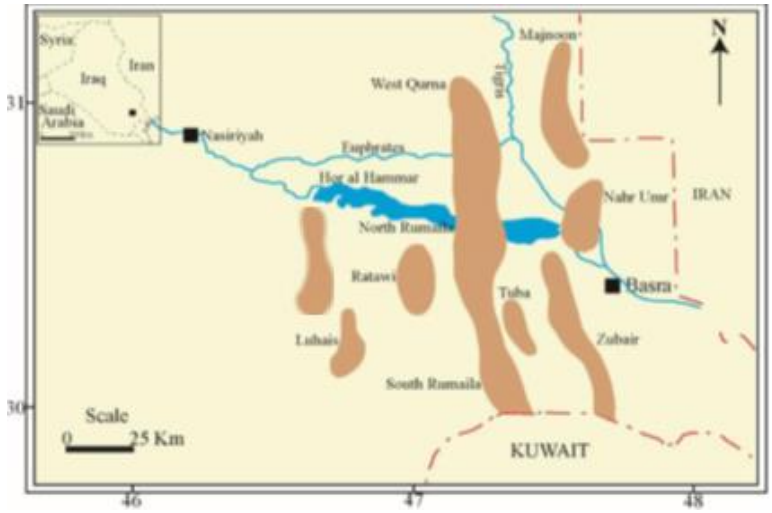

Fig. (1): Study field map location [14].

2. Material and Method

2.1. Fluid Modeling

The PVT data are available for the X oil field in well W-4 taken midway through 1987 for the Y formation, the sample shows that the crude is medium oil with stock tank gravity of 28.8 API and with an initial GOR of 61.91 $m^3/m^{3.}$. The bubble point of the sample of 1102.7 psia at 82.8 C. The PVT report's study of the reservoir fluid composition, which is cited in Table (2), came from the laboratory at a temperature of 82.8 C, molecular weight of $C6^+$ of 234, and specific gravity of 0.8994.

Table (2): The Composition of Reservoir Fluid Sample for well W-4 [15]

Components	Mole
N_2	0.31
CO_2	0.16
C_1	16.51
C_2	8.33
C_3	8.46
i-C_4	1.76
n-C_4	4.98
i-C_5	2.21
n-C_5	2.87
C_6^+	54.41
Total	100

The reservoir fluid was characterized and phase behavior was examined using CMG WinProp software. To examine the phase behavior of the reservoir fluids, a tailored PVT model was created. Selecting the Peng Robinson Equation (1) of State (1978) was the initial step. Constant Composition Expansion (CCE), Differential Liberation (DL), and compositional analysis of experimental data

were utilized as matching points for the CMG WinProp program [16,17].

$$P = \frac{RT}{V-b} - \frac{a\alpha}{V(V+b)+b(v-b)} \dots\dots\dots\dots\dots\dots\dots\dots\dots\dots\dots\dots\dots\dots\dots\dots (1)$$

Where:

$$a = \frac{\Omega_a (RT_C)^2}{P_C} \quad , b = \frac{\Omega_b RT_C}{P_C} \quad , \Omega_a = 0.457235 \, , \Omega_b = 0.077796$$

$$\alpha = a\alpha \ , \quad \alpha^{\frac{1}{2}} = 1 + m\left(1 - T_r^{\frac{1}{2}}\right), \quad T_r = \frac{T}{T_C},$$

$$m = 0.37464 + 1.54226\omega - 0.26992\omega^2$$

Where, P = pressure (Psia), R= Gas Constant, (psia.ft3)/ (lb.mole. R), V=Volume, (ft3), a, b, = Constants in various equations of state, (dimensionless), Ω=Equation of state parameter, (dimensionless), ω=Acentric factor, (dimensionless), α=Equation of state parameter, (dimensionless), Tc=Critical Temperature, (R), Pc=Critical Pressure, (Psia), Tr=Reduce Temperature, (dimensionless).

2.2. MMP Estimation

The model was calibrated and adjusted, and then the Semi-analytical (Key Tie Lines) method was used to estimate the MMP, Since the GMG group recommends it as a high close result to experimental values, it is the preferred approach over the others. Because analytical techniques rely on precise liquid characterization via an equation of state (EOS), they are extremely quick. Analytical approaches are very promising for the creation of optimal fluid couplings and for use in synthesized rheological simulations because of their increased speed. Whenever the pressure is raised, the MMP happens when any of the main tie lines first crosses a critical point or reaches zero length [18].

With an emphasis on key tie lines, the approach entails studying ternary systems to assess miscibility. In the two-phase area along a dilution line, injection gas and initial oil are mixed to start the process. Then, using an equation of state, the equilibrium compositions of the liquid and vapor phases are determined. The operation is contained until the liquid and vapor compositions converge, showing the tie line extending through the initial oil composition. The vapor phase is combined with more original oil. This iterative procedure is called forward contacts as shown in Figure (2).

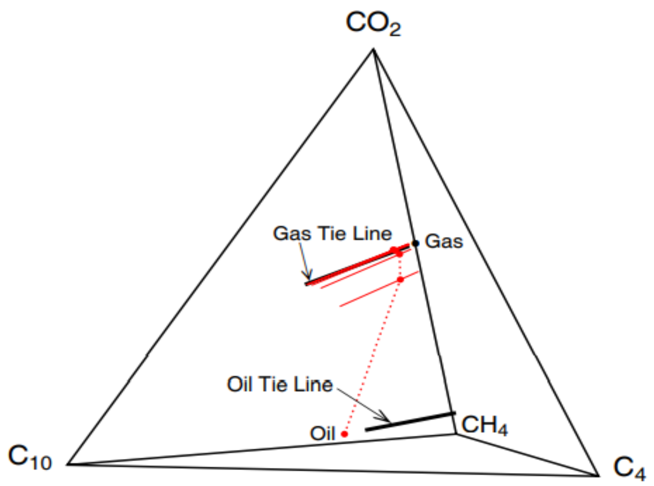

Fig. (2): Tie Lines and Composition Route for Oil Reversal Contacts [19]

2.3. Solubility

There are three main ways that deep saline aquifers, which make up a sizable portion of sedimentary basins by volume, can sequester or store carbon dioxide: (a) solubility trapping, which involves allowing the gas to dissolve in the formation water; (b) mineral trapping, which involves allowing the gas to dissolve in the rocks and aquifer fluids; and (c) trapping of the hydrodynamic CO_2 plume. Apart from related oil and gas reservoirs, a CO_2 plume could also be caught in stratigraphic and/or geological traps along a flow channel. As a result, the capacity of a deep, saline aquifer can be taken into account for CO_2 that is converted to rock matrix, CO_2 phase dissolved in formation water, and free-phase CO_2 in the pore space. Henry's Law is used to model solubility in the water phase. There are two versions accessible [20; 21].

1. The principle of Henry's Law, which applies the fugacity formula given below:

$$F = X * H \quad \ldots\ldots (2)$$

Where, f=component fugacity, X= component composition in aqueous phase; H= constant of Henry's.

The following formula yields constants of Henry's Law, H, at all pressures, p:

$$\ln(H) = \ln(hens) + V8*(Pref)/RT \quad \ldots\ldots (3)$$

Where, hens = Actual Numbers for the purpose of reference Henry's law constants for the components at a reference pressure Pref (kPa/psia). Zero for insoluble components in water, V8= the components' partial molar volume in water at infinite dilution, expressed in units of (L/mol).

2. When solubility is taken to be ideal, the simplified version of Henry's Law simplifies ideal gas,

which leads to the following assumption.

$$Z * P = X*H \quad \text{.....(4)}$$

Where, Z= is the global hydrocarbon phase composition in relation to the aqueous phase, P = pressure.

In CMG-GEM when the Henry correlation is specified, the reference pressure Pref corresponds to the pressure saturation for water at a given temperature, and the reference Henry's constant (hens) is correlated using Harvey's (1996) work. For molar volume at infinite dilution, further temperature-dependent correlations are employed (V8). After that, the Henry's-constant H is found using the formula mentioned in Equation (3) above [21].

3. Results and Discussion:

3.1. PVT Model Matching:

Several attempts were made to get a match for all the parameters by tuning EOS without splitting the pseudo component by manipulation of critical properties of the pseudo component. The process of fine-tuning the EOS involved many regressions. Every experiment was run against the critical pressure of the pseudo components, $C6^+$, in the first regression. When the findings were tested against PVT data, they produced highly accurate forecasts with minimal error.

The $C6^+$ pseudo components critical pressure (Pc), critical temperature (Tc), a centric factor (ω), and binary interaction coefficients (δ) were essentially the regression parameters. Additionally, the shift parameters of the $C6^+$ pseudo components were regressed collectively to ensure consistency in changes within the $C6^+$ fraction. The optimal EOS regression parameters for Y reservoir fluid are listed in Table (2) following:

Table (3): Optimal Regression Equations and Crucial Characteristics for Y Reservoir.

Comp.	Pc (atm)	Tc (K)	Acentric Factor (ω)	Mol. weight	Vol. shift	Omega A	Omega B
N_2	33.5	126.2	0.04	28.013	-0.1927	0.457235	0.0777960
CO2	72.8	304.2	0.225	44.01	-0.0817	0.457235	0.0777960
CH4	45.4	190.6	0.008	16.043	-0.4595	0.457235	0.0777960
C2H6	48.2	305.4	0.098	30.07	-0.3134	0.457235	0.0777960
C3H8	41.9	369.8	0.152	44.097	0.11369	0.457235	0.0777960
IC4	36	408.1	0.176	58.124	0.1156	0.457235	0.0777960
NC4	37.5	425.2	0.193	58.124	-0.0675	0.457235	0.0777960
IC5	33.4	460.4	0.227	72.151	-0.0608	0.457235	0.0777960
NC5	33.3	469.6	0.251	72.151	-0.039	0.457235	0.0777960
C6+	17.92	950.26	0.30643464	234.0099	0.27876193	0.457235	0.0777960

The comparison of the outcomes of certain experiments is shown in Figures (3) to (5), demonstrating the statistical correctness between the measured and final findings of Constant Composition Expansion and Differential Liberation data. As can be shown, for every parameter, the findings showed an excellent fit with the measured values.

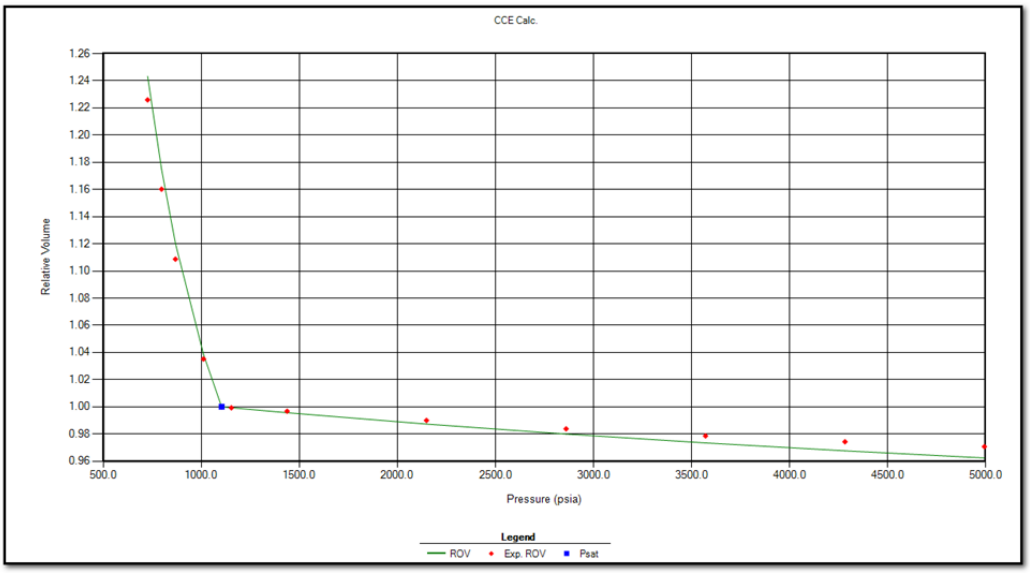

Fig. (3): Comparing the Expected and Observed Relative Volume Values.

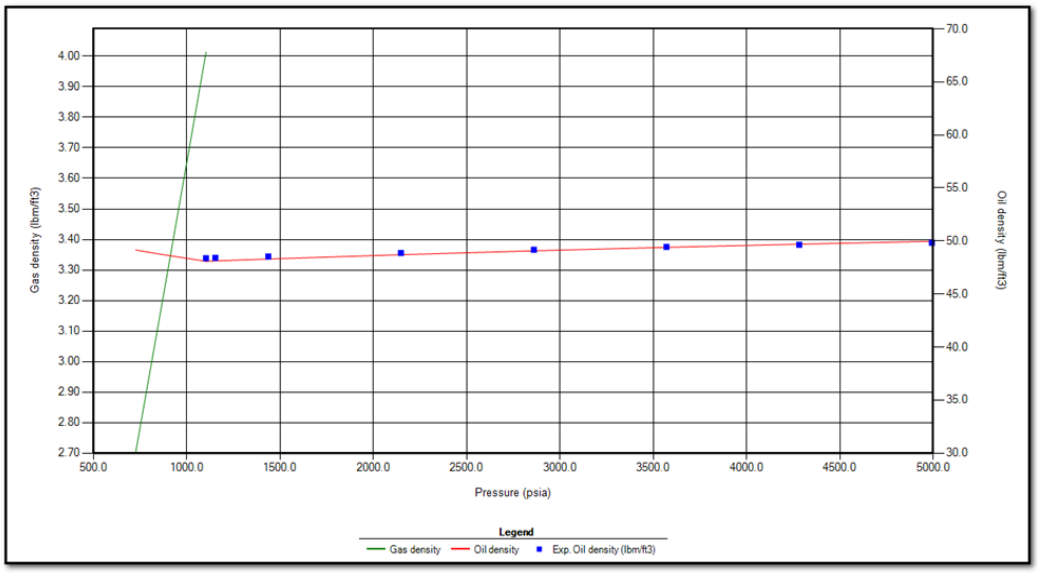

Fig. (4): Comparing the Expected and Observed Gas Density.

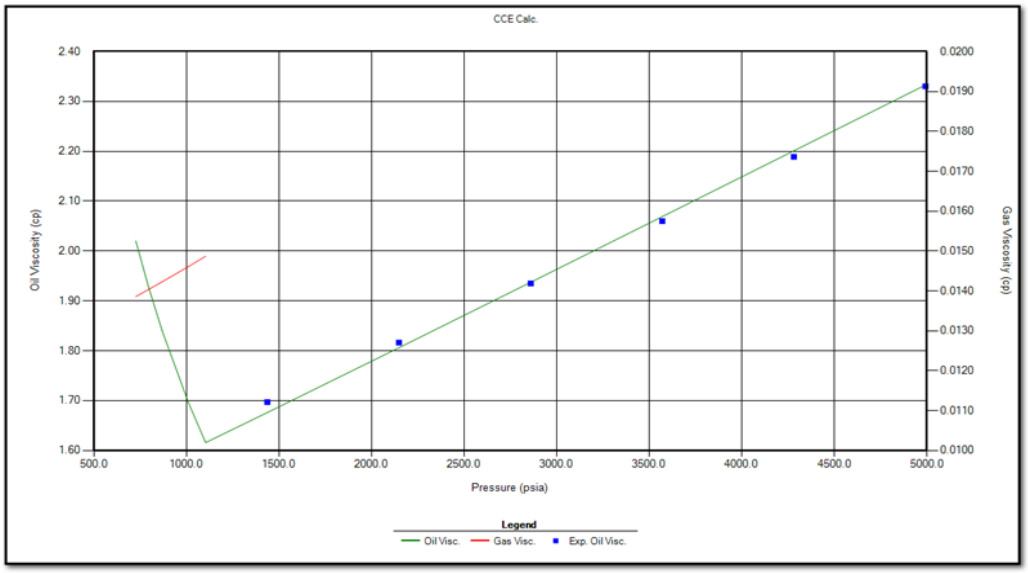

Fig. (5): Comparing the Expected and Observed Oil Viscosity.

3.2. MMP and FCM Estimation:

The WinProp Multi-Contact Miscibility (MCM) option can also be used to determine the minimum miscibility enrichment level (MME) needed for multiple or single contact miscibility at a particular temperature, pressure, oil composition, primary and make-up gas compositions, as well as a minimum miscibility pressure (MMP) or first contact miscible pressure (FCM) for a provided oil and solvent at a given temperature.

By inputting an array of pressures that will be tested, the lowest miscibility pressure for a certain solvent composition may be found. Figure (6) the injection of CO_2 displays the results from the first and multiple contact calculations for the Nahr Umer reservoir. For CO_2 injection, the MMP result is 2100 psia.

```
*************************************************
*                                               *
*               WINPROP  2018.10                *
*            2015-May-22   09:59:51             *
* Computer Modelling Group Ltd., Calgary, Canada *
*                      20                       *
*************************************************
Multiple contact calculations

SUMMARY OF FIRST CONTACT MISCIBILITY
CALCULATIONS AT TEMPERATURE =    181.040 deg F

FIRST CONTACT MISCIBILITY PRESSURE
(FCM) IS GREATER THAN  4014.7  psia


SUMMARY OF MULTIPLE CONTACT MISCIBILITY
CALCULATIONS AT TEMPERATURE =    181.040 deg F

MULTIPLE CONTACT MISCIBILITY ACHIEVED
AT PRESSURE =  2100.87  psia
MAKE UP GAS        MOLE FRACTION =  0.00000E+00
BY VAPORIZING AND CONDENSING COMBINED GAS DRIVE
*************************************************
```

Fig. (6): Result of FCM and MMP for Y Formation.

3.3. Reservoir Model

After the completion geological model for Y formation, the final version model was modified to reduce the total Number of cells using grid upscaling with scale-up structure (reducing the Number of layers) and scale-up properties. The produced model with 123 cells in the X direction, 353 cells in the Y direction, and 13 cells in the Z direction, so the total Number of cells is 564,447 cells. Then this model is exported as a Rescue File that can be read in CMG software and the GEM simulator is used to run the simulation model for Y formation as shown in Figure (7).

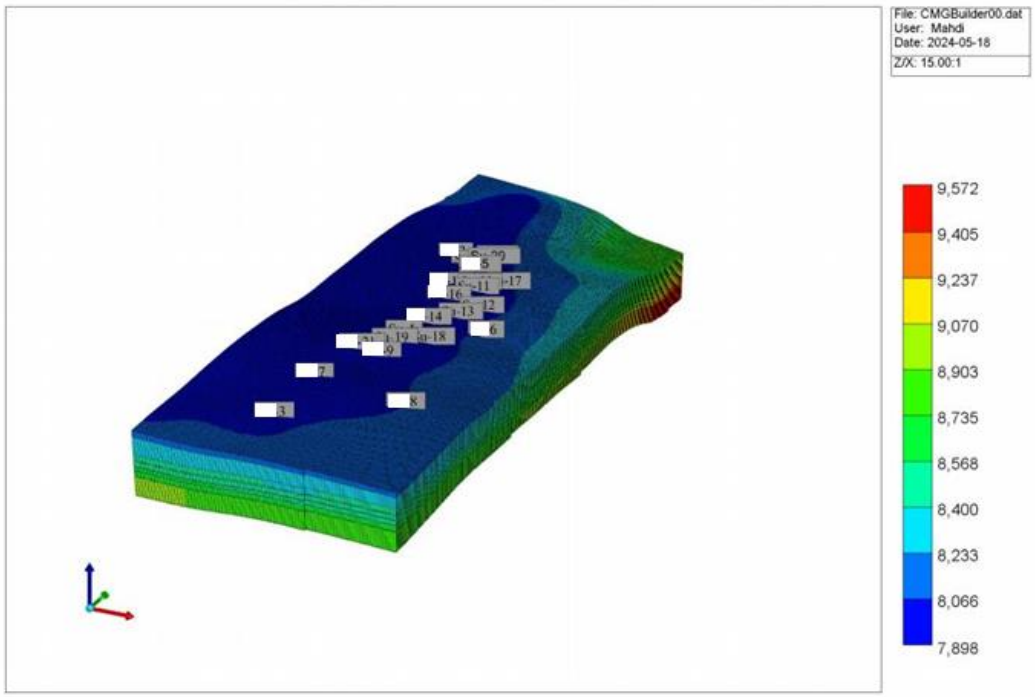

Fig. (7): Exported Model for Y Formation in CMG

Because this study includes CO_2 injection, it is important to find the fracture pressure for Y formation to consider it as one of the important constraints, so the next sections focus on preparing the required data for run simulation.

3.4. Fracture Pressure

This step comprises the computations for hydrostatic pressure, pore pressure, fracture pressure, lithology discrimination, and overburden stress using logs data including (resistivity, neutron-porosity, density, gamma ray, Shear slowness, and compressional slowness logs) run in well W-20. In order to distinguish between shale and non-shale intervals, gamma-ray logs are utilized [22]. The overburden stress was computed using the density log, and using pore pressure to compute effective

vertical stress. Then Eaton and Eaton (1997) used to calculate fracture pressure using Techlog software with 6048 psia as shown in Figure (8) [23].

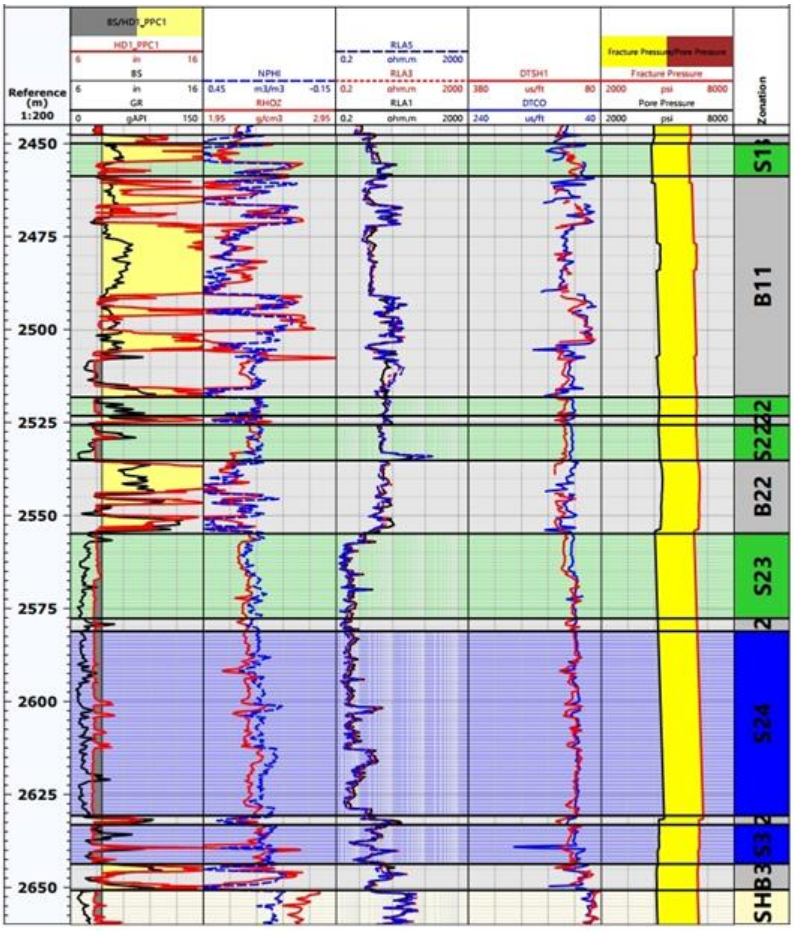

Fig. (8): Fracture pressure for Y Formation W-20

3.5. Vertical Permeability

The recent core sample was taken from Y formation from well W-23 and performed vertical and horizontal permeability measurements, the results showed that the vertical to horizontal permeability with the value of 21 % as shown in Table (4).

Table (4): Vertical to Horizontal Permeability Ratio for Y Formation

Depth	K_v	K_h	K_v/K_h	Avg. (K_v/K_h)
2528.75-2528.88	78.85	214.944	0.36684	0.21654948
2530.65-2530.79	158.72	1319.47	0.120291	**22%**
2539.26-2539.15	241.941	1488.703	0.162518	

3.6. Water Solubility

The method used for calculating water solubility data was explained in section three (3.3), the resulting data is cited in Table (5) below, and the Henry's constant taken a value just for CO_2 to activated soluble active in water with the Henry's constant of 1 E+20 to make the components insoluble.

Table (5): Aqueous Phase Solubility Data for Y Formation

Components	Henry's constant (psi)	Ref. Pressure (psi)	V-infinity (m^3/kgmole)
N_2	1e+20	4.0785000E+03	3.2208778E-02
CO_2	8.6772657E+04	4.0785000E+03	3.5415974E-02
CH_4	1e+20	4.0785000E+03	3.5569287E-02
C_2H_6	1e+20	4.0785000E+03	5.2235355E-02
C_3H_8	1e+20	4.0785000E+03	7.1644052E-02
I-C_4	1e+20	4.0785000E+03	9.1213802E-02
N-C_4	1e+20	4.0785000E+03	9.1233725E-02
I-C_5	1e+20	4.0785000E+03	1.1030010E-01
N-C_5	1e+20	4.0785000E+03	1.1277656E-01
C_6^+	1e+20	4.0785000E+03	4.1610243E-01

3.7. CO_2 Availability

The CO_2 emission from a different source was not accurately measured in one south governorate so to make this study as soon as possible near to the actual Status of the daily amount of CO_2 emission in National Oil Company calculated by MoO for years (2018-2019-2020) as cited in the Table (6) below [24].

Table (6): Daily CO_2 Emission in NOC

Year	Daily CO_2 (Ton)	Daily CO_2 (scf)
2018	7934	152,923,688
2019	6480	124,898,601
2020	2701	52,060,358

So, the injection rate of CO_2 was selected according to the lower value of emission in 2020. The table above does not include the emissions from the Refinery, power stations, and other emission sources.

3.8. History Matching

The simulation model used for the run compositional model for Y formation should conform to the model valid and represent the reservoir so the history match must be performed for production and pressure data. In the X oil field, there is a challenge of leaks in both pressure and production. The X field put on production through an early production period from February 1990 to August 1990 from wells (W-4, W-5, W-11) from Y formation. In this period the production data recorded only include the total volume of oil produced from both reservoirs (Y, B) with on pressure and water cut record and total oil produced of 832 Mstb. However, in January 2018 the production from the Y formation was resumed, and also the production volume of oil was recorded only for both reservoirs and later the field again shut down because of a high water cut.

The purpose of the matching procedure was to match well W-4's bottom hole pressure. On December 5, 1978, W-4 underwent an open-hole drill-stem test (DST). The available data is a brief synopsis that includes the well productivity index (PI) and static formation pressure. The first and second build-up tests are the two primary build-up tests found in the DST test. The first build-up lasts for 45 minutes, from 10:10 to 10:55, and the second build-up lasts for 55 minutes, from 11:40 to 12:35. To achieve the best match between the calculated bottom-hole pressure (BHP) in the model and the recorded BHP, numerous attempts were made with the model. The best matching results are obtained by multiplying the permeability in the J-direction by 3, as illustrated in Figures (9) and (10) Figure (11) illustrates the production history matching that was accomplished for field production throughout the experimental period and later after obtaining an acceptable pressure history matching.

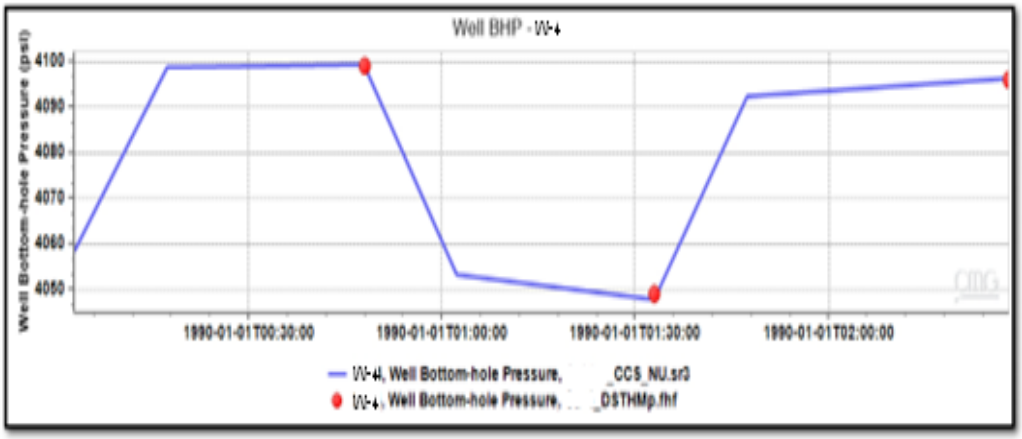

Fig. (9): History Match Pressure W-4 DST

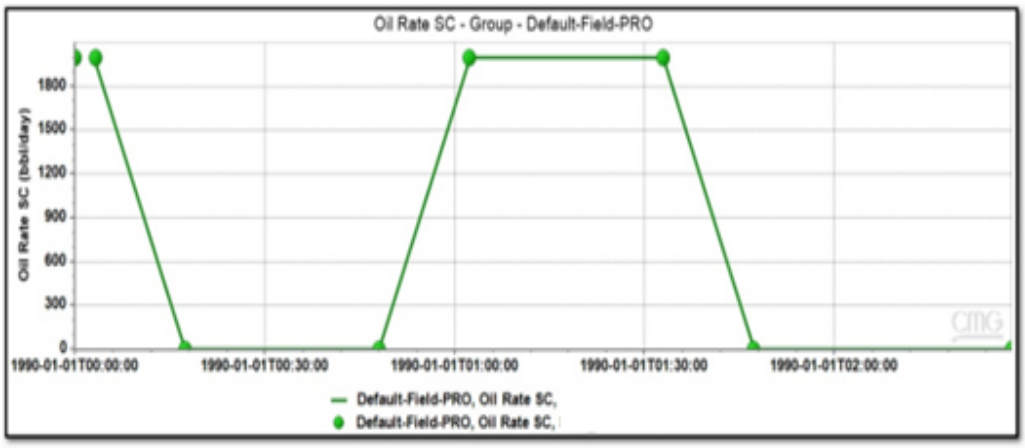

Fig. (10): History Match Flow Rate W-4 DST

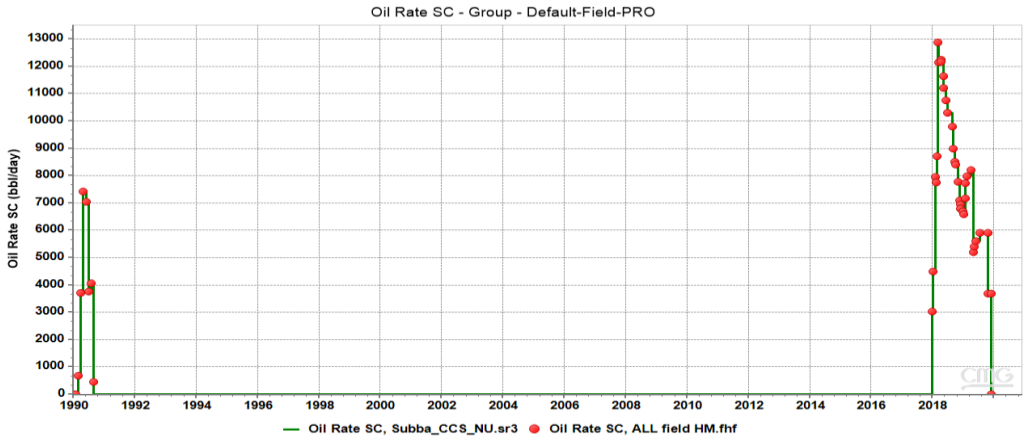

Fig. (11): Accumulation Oil Production History Match

Figures (12), (13), (14), and (15) show the history match for wells produced through the trail production and later approximated according to the productivity index for each well.

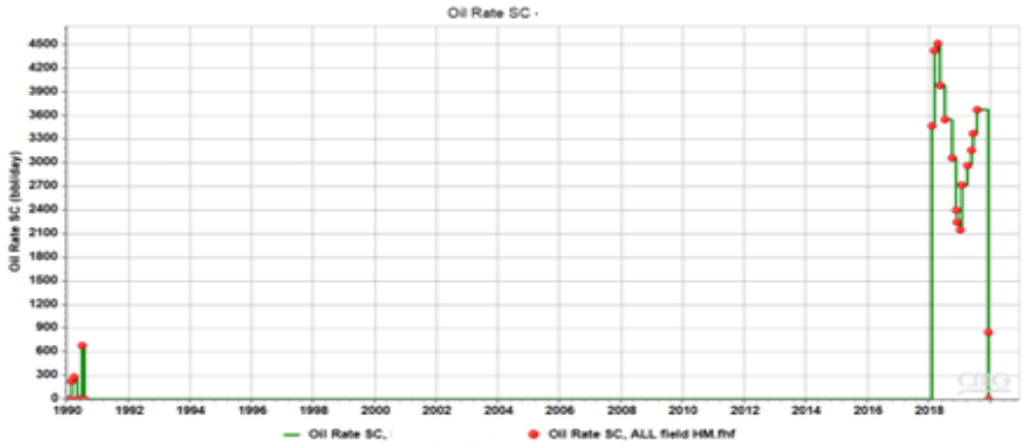

Fig. (12): History Match Flow Rate for Well W-4

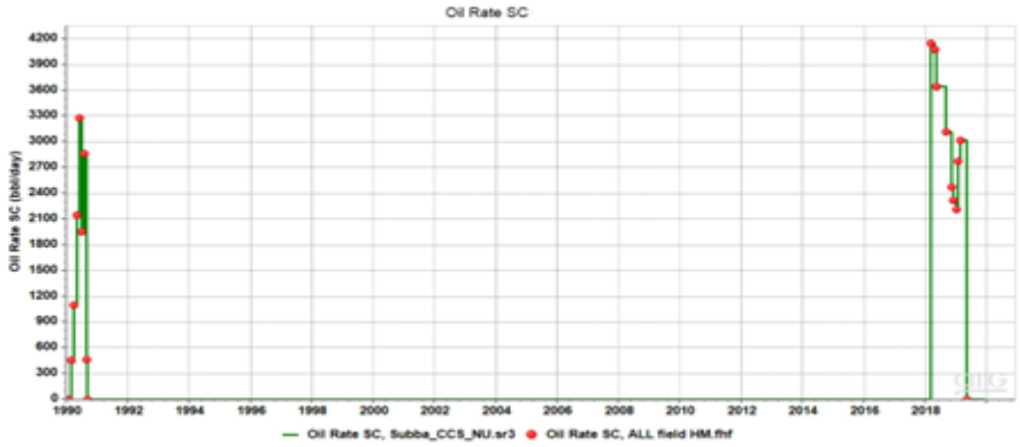

Fig. (13): History Match Flow Rate for Well W-5

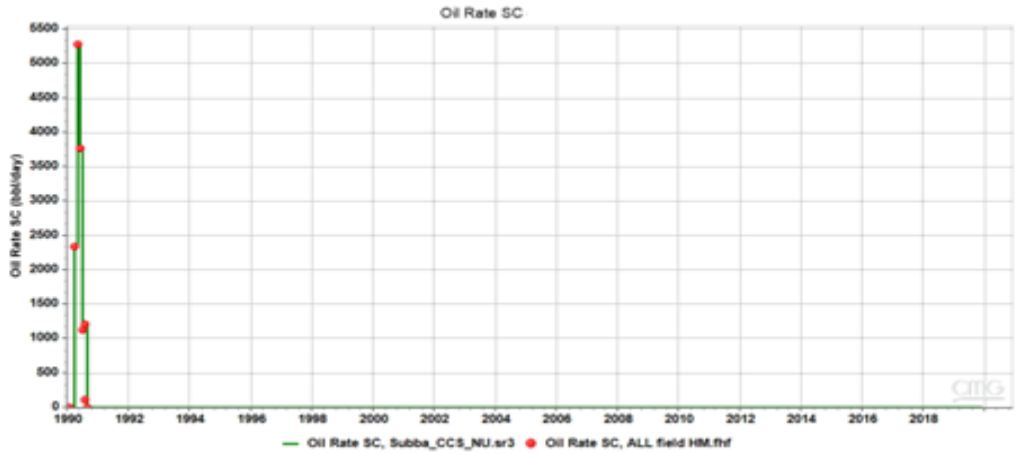

Fig (14) History Match Flow Rate for Well W-11

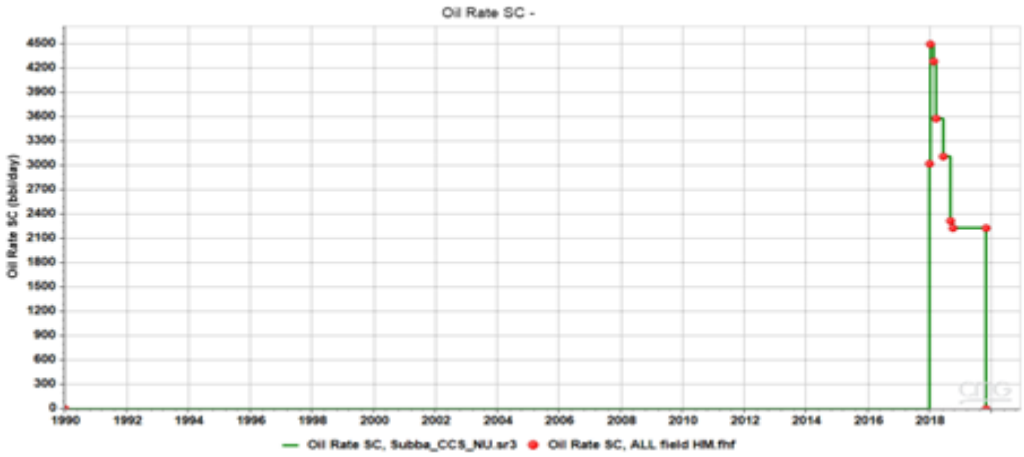

Fig. (15): History Match Flow Rate for Well W-16

3.9. Prediction Case of Five-Spot CO_2 Injection

In this case, the oil produced from layer S21 through 17 production wells and 21 injection wells to achieve 30 kstb/day. The injection rate of CO_2 of 42 mmscf/day begins after 5 years after the start of commercial production, then after the breakthrough, the rate of injection was reduced to 21 mmscf/day at the same time starting the injection of CO_2 in the aquifer (S24, S3) as a sequestration project through abandonment wells (W-3, W-6, W-8). The target of 30 kstb/day sustained for 20 years from 2025 to 2045 with pressure above Pb and WC less than 0.65%. The production strategy in this case starts production from existing wells (W-5, W-20) and adds production well every two months. The accumulation result of oil production at the end of the simulation was 260 MMstb, as shown in Figures (16) and (17).

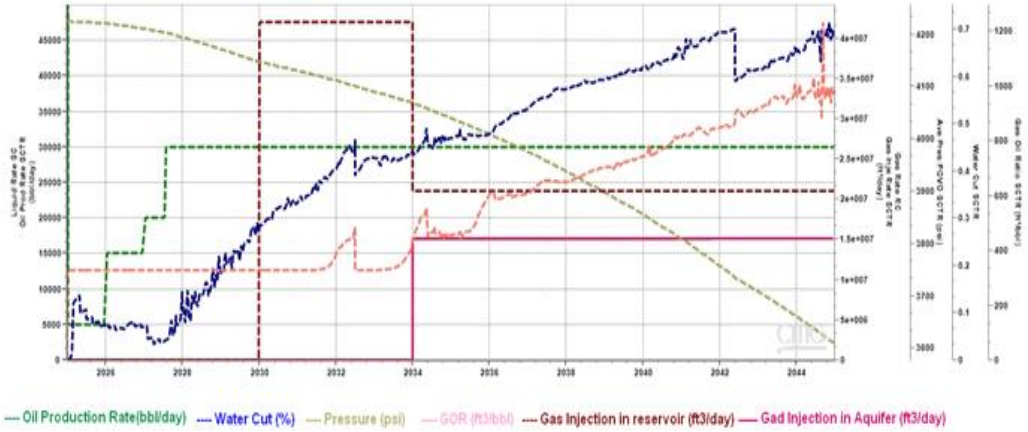

Fig. (16): Results of Simulation Case with 5-Spot Vertical Wells CO_2 Injection

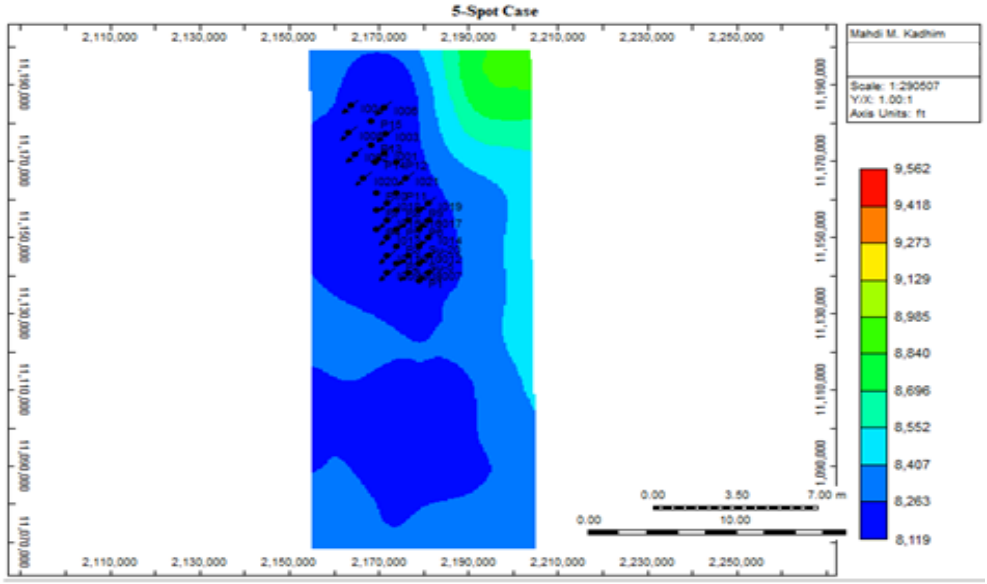

Fig. (17): Wells Location of 5-Spot Vertical Wells Injection Case

The comparison of all cases shown the Case with 5-Spot Vertical Wells CO2 Injection appears high cumulative oil production and a minimum Number of wells. All cases show high recovery compared to natural depletion using CO_2 injection except the Case-4 7-spot injection, additionally, the drilling of horizontal wells in this type of formation will be face many problems and lead to uneconomical development. The WC in all cases showed high and rapidly increasing results from high vertical permeability. All this reason makes 5-spot vertical well CO_2 injection the preferred method to develop Y formation in X oil field. Table (7) shows the comparison between all cases.

Table (7) Comparing Import Parameter for All Cases

No.	Case	No. Of Production Wells	No. Of Injection Wells	CO_2 Injection Rate MM (Ft3/D)	Oil Production Rate (Stb/D)	Duration (Year)	Max WC (%)	Cumulative oil production (MMstb)	Recovery Factor (%)
1	Natural depletion	14	0	0	30,000	8	0.6	106	7
2	5-spot	17	21	42 – (21+15)	30,000	20	0.6	260	17.3
3	5-spot-Horizontal	17 (Horizontal)	21	45	30,000	19.1	0.6	258	17.2
4	7-spot	15	52	45	30,000	13.5	0.6	186	12.4
5	Direct line spot	36	36	45	30,000	18	0.6	245	16.3
6	Peripheral spot	14	15	45	30,000	10.5	0.6	146	16.4

3.10. CO_2 Sequestration Through EOR Process

The CO_2 injection in layer S21 started in 2030 after five years of starting commercial production with the rate of 42 MMscf/day through 21 injection wells then the rate was reduced to 21 MMscf per day after the breakthrough reached (1/1/2034). At the end of the simulation (1/1/2045). At the total amount of CO_2 stored in the oil zone of 5,750,630.38 Tons, as shown in Figures (18) and (19) below.

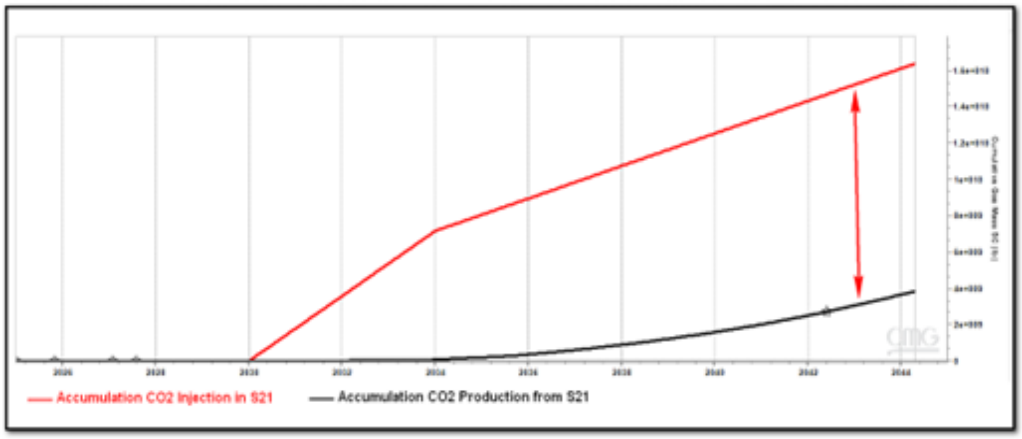

Fig. (18): Accumulation of CO_2 Injection and Production in the Unit S21

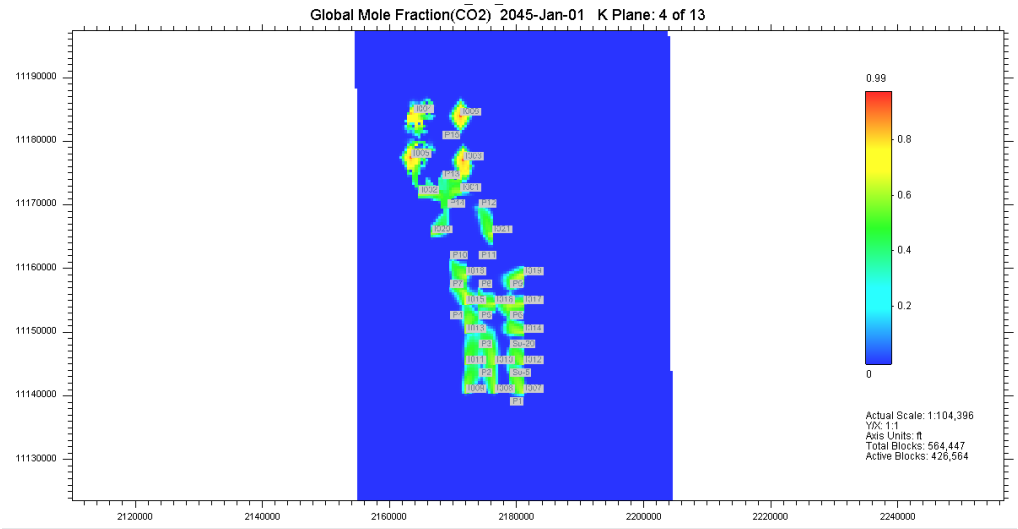

Fig. (19): Mole Fraction of CO_2 at the End of Simulation Time in the Unit S21

In the aquifer units (S24, S3), the CO_2 starts injection in 1/1/2034 using 3 abandonment wells (W-3, W-6, W-8) with the rate of 15 MMscf/day. At the end of the simulation, the total amount of CO_2 stored and soluble in the aquifer of 3,265,306.12 Tons as shown in Figures (20), (21), and (22) below.

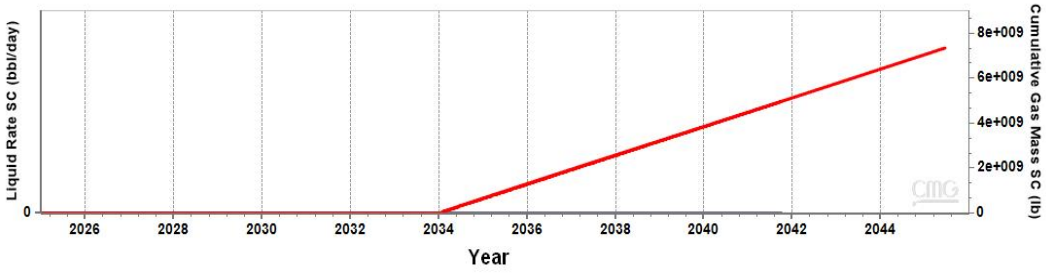

Fig. (20): Accumulation of CO_2 Injection in the Units S24 and S3

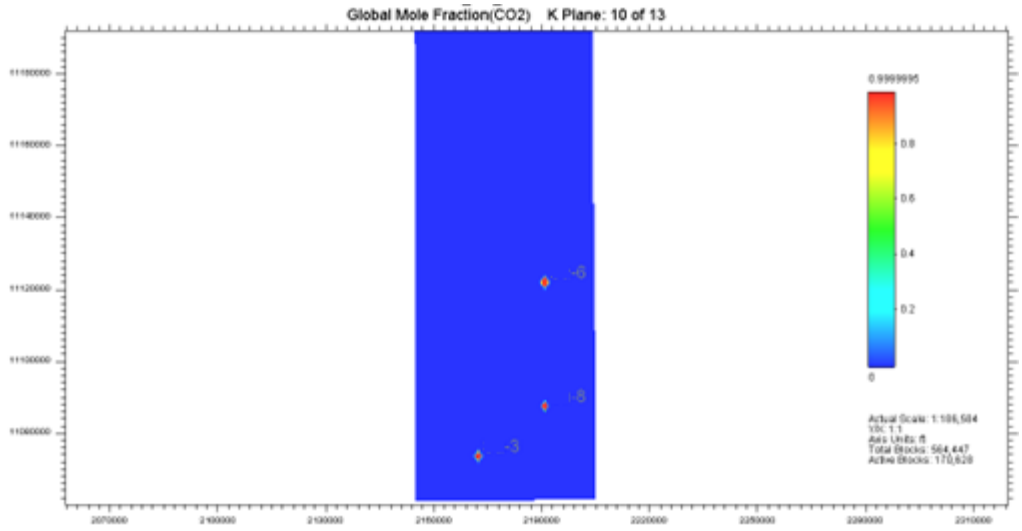

Fig. (21): Mole Fraction of CO_2 at the End of Simulation Time in the Unit S24

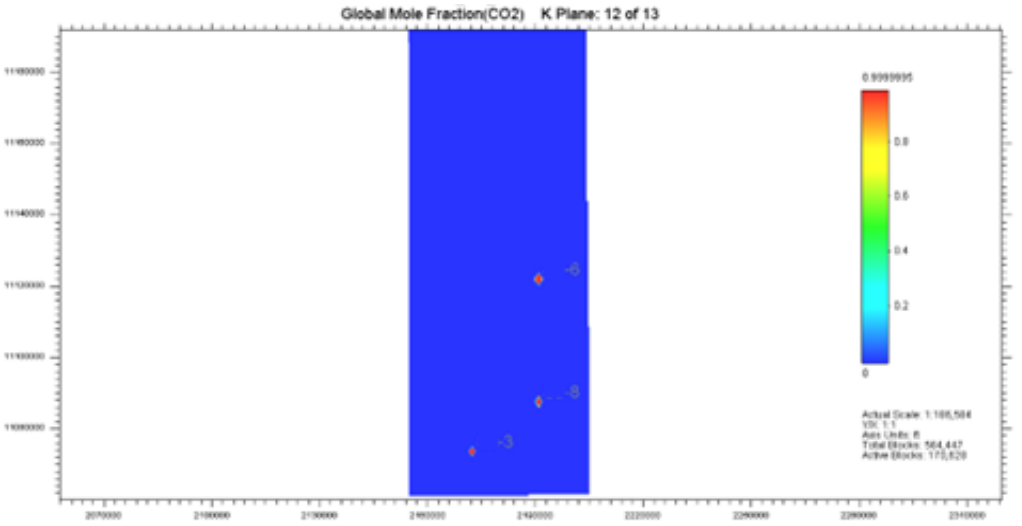

Fig. (22): Mole Fraction of CO_2 at the End of Simulation Time in the Unit S3

4. Conclusions

The following succinctly describes the primary findings of the present study:

1. PR-EOS was effectively adjusted to match experimental results obtained via differential liberation and constant composition expansion. For the experiment's bubble point pressure, and gas oil ratio, which is also liquid density, a good match with PR-EOS was achieved. After conducting calculations and simulations to ascertain the MMP of the reservoir fluid in the Y formation, Winprop-2018's Semi-analytical (Key Tie Lines) method simulation was found to be the nearest and validated method when compared to existing empirical correlations, as well as the fastest and most economical when compared to other suggested techniques.

2. The 5-Spot CO_2 injection continuous through production layer S21 appear high cumulative oil production and the minimum Number of wells with 260 MMstb and (17 + 21) wells with a recovery factor of 17.3 %. The plateau of oil reached 30 Kstb/d for 20 years starting in the year of 2025 with existing wells (W-5, W-20) and adding production well every two months.
3. The 5-Spot horizontal wells case showed a near recovery factor to the based case but there are a lot of challenges with drilling horizontal wells in this type of formation, additionally the direct line and peripheral spot exhibited high recovery but with an increase in the Number of wells and still lower recovery than based case.
4. Injection of CO_2 miscible in unit S21 leads to storing in an oil zone of 5,750,630.38 Tons at the end of the simulation case.
5. The aquifer in the Y formation with barriers makes it a shoutable condition as storage for CO_2 with the rate of 15 MMscf/d through abandonment wells to decrease the additional cost of drilling wells for this purpose, so the total amount of CO_2.

Nomenclatures

NOC	National Oil Company
3D	Three-Dimension
CMG	Computer Modelling Group
CCUS	Carbon Capture, Utilization and Storage
EOR	Enhanced Oil Recovery
API	American Petroleum Institute
CCE	Constant Composition Expansion
DL	Differential Liberation
MMP	Minimum Miscible Pressure
EOS	Equation Of State
PVT	Pressure-Volume-Temperature
FCM	First Contact Miscible Pressure
MoO	Ministry Of Oil
BHP	Bottom-Hole Pressure
DST	Drill Stem Test

Author Contribution Statement: All authors contributed to the conception and research design of the study, data collection and processing, data analysis and interpretation, literature review, drafting of the manuscript, and revision and proofreading. All authors have read and approved the final version of the manuscript.

References

[1] L. S. Melzer, "Carbon dioxide enhanced oil recovery (CO2 EOR): Factors involved in adding carbon capture, utilization and storage (CCUS) to enhanced oil recovery", *Center for Climate and Energy Solutions*, p9. 1-17, 2012.

[2] T. A. Jelmert, N. Chang, and L. Høier, *"Comparative study of different EOR methods"*, 2010.

[3] M. Latil, C. Bordon, J. Burger, and P. Sourieau, *"Enhanced Oil Recovery"*, Gulf Publ. Co., London, 1980.

[4] A. Bashir, M. Ali, S. Patil, M. S. Aljawad, M. Mahmoud, D. Al-Shehri, H. Hoteit, and M. S. Kamal, "Comprehensive review of CO2 geological storage: Exploring principles, mechanisms, and prospects*"*, *Earth-science Reviews*, vol. 249, p. 104672, 2024. https://doi.org/10.1016/j.earscirev.2023.104672

[5] F. M. Orr, "Storage of Carbon Dioxide in Geologic Formations", *Journal of Petroleum Technology*, vol. 56, no. 09, pp. 90–97, Sep. 2004. https://doi.org/10.2118/88842-JPT

[6] B. Saberali, N. Golsanami, K. Zhang, B. Gong, and M. Ostadhassan, "Simulating dynamics of pressure and fluid saturation at grid-scale by a deep learning-based surrogate reservoir modeling based on a fast-supply hybrid database and developing preliminary insights for future gas hydrate exploitations in China", *Geoenergy Science and Engineering*, vol. 222, p. 211415, 2023. https://doi.org/10.1016/j.geoen.2023.211415.

[7] X. Wang, S. Li, B. Tong, L. Jiang, P. Lv, Y. Zhang, Y. Liu, and Y. Song., "Multiscale wettability characterization under CO_2 geological storage conditions: A review", *Renewable & Sustainable Energy Reviews*, vol. 189, p. 113956, Jan. 2024. https://doi.org/10.1016/j.rser.2023.113956.

[8] M. Dong, H. Gong, Q. Sang, X. Zhao, and C. Zhu, "Review of CO_2-kerogen interaction and its effects on enhanced oil recovery and carbon sequestration in shale oil reservoirs", *Resources Chemicals and Materials*, vol. 1, no. 1, pp. 93–113, Mar. 2022. https://doi.org/10.1016/j.recm.2022.01.006.

[9] H. W. L. Rodrigues, E. J. Mackay, and D. P. Arnold, "Multi-objective optimization of CO2 recycling operations for CCUS in pre-salt carbonate reservoirs", *International Journal of Greenhouse Gas Control*, vol. 119, p. 103719, Sep. 2022. https://doi.org/10.1016/j.ijggc.2022.103719.

[10] L. Zhang, B. Ren, H. Huang, Y. Li, S. Ren, G. Chen, and H. Zhang, "CO_2 EOR and storage in Jilin oilfield China: Monitoring program and preliminary results", *Journal of Petroleum Science and Engineering*, vol. 125, pp. 1–12, Jan. 2015. https://doi.org/10.1016/j.petrol.2014.11.005.

[11] X. Lyu and D. Voskov, "Advanced modeling of enhanced CO_2 dissolution trapping in saline aquifers", *International Journal of Greenhouse Gas Control*, vol. 127, p. 103907. 2023. https://doi.org/10.1016/j.ijggc.2023.103907.

[12] P. S. Kang, J. S. Lim, and C. Huh, "Screening Criteria and Considerations of Offshore Enhanced Oil Recovery", *Energies*, vol. 9, no. 1, p. 44, Jan. 2016. https://doi.org/10.3390/en9010044.

[13] D. W. Green, and G. P. Willhite, *"Enhanced Oil Recovery", SPE, 2nd. Ed*, TX, 1998.

[14] M. I. Salman and T. A. Mahdi, *"A Comparative Reservoir Study of Zubair and Y Formations in X Oilfield, Southern Iraq*" Iraqi Geological Journal, vol. 56, no. 2F, pp. 186–203, 2023. https://doi.org/10.46717/igj.56.2F.12ms-2023-12-18.

[15] PVT report for wells W-4, *Ministry of Oil*,1987.

[16] H. Yuan, and T. R. Johns, "Simplified method for calculation of minimum miscibility pressure or enrichment", *SPE Journal*, vol. 10, no. 4, pp. 416–425. 2005. https://doi.org/10.2118/77381-PA

[17] H. F. Al-Khafaji, Q. Meng, W. Hussain, R. K. Mohammed, F. Harash, and S. A. AlFakey, "Predicting minimum miscible pressure in pure CO2 flooding using machine learning: Method comparison and sensitivity analysis", *Fuel*, vol. 354, p. 129263. 2023. https://doi.org/10.1016/j.fuel.2023.129263

[18] M. F. Orr, *"Theory of gas injection processes"*, Tie-Line Publications, 2007.

[19] L. W. Holm and V. A. Josendal, "Mechanisms of Oil Displacement by Carbon Dioxide", *Journal of Petroleum Technology*, vol. 26, no. 12, pp. 1427–1438, 1974. https://doi.org/10.2118/4736-PA

[20] Y. Li and L. X. Nghiem, "Phase equilibria of oil, gas and water/brine mixtures from a cubic equation of state and henry's law", *Canadian Journal of Chemical Engineering*, vol. 64, no. 3, pp. 486–496, 1986. https://doi.org/10.1002/cjce.5450640319

[21] A. H. Harvey, "Semiempirical correlation for Henry's constants over large temperature ranges", *AIChE Journal*, vol. 42, no. 5, pp. 1491–1494, 1996. https://doi.org/10.1002/aic.690420531

[22] M. D. Matthews, "Uncertainty-shale pore pressure from borehole resistivity", *In ARMA North America Rock Mechanics Symposium*, pp. ARMA-04-551, 2004.

[23] Eaton, B.A. and Eaton, T.L. "Fracture gradient prediction for the new generation", *World Oil*, vol. 218, no. 10, pp.93-97. 1997.

[24] M. K. Nashwan, "Study of gas emissions amount estimation in the Iraqi oil companies for years (2018,2019,2020)", *Ministry of Oil, Studies and Planning and Follow Up Directory*, 2021.